FIRST MEASUREMENT RESULTS AT THE LEG PROJECT'S 100 keV DC GUN TEST STAND

S. C. Leemann, Å. Andersson, R. Ganter, V. Schlott, A. Streun, A. F. Wrulich,
PSI, Villigen, Switzerland

Abstract

The Low Emittance Gun Project (LEG) at PSI [1] aims at developing a high-brightness, high-current electron source: a 20-fold improved brightness compared to present state-of-the-art electron guns. The source is intended to form the basis for a cost-efficient implementation of a high-power X-ray FEL light-source for scientific research at PSI. A field emitter array (FEA) cathode is being considered a source candidate. In order to study pulsed field emission from such a cathode and to investigate space charge compensation techniques as well as to develop diagnostic procedures to characterize the beam resulting from an FEA cathode, a 100 keV DC gun test stand has been built. The test stand gun and diagnostics have been modeled with the codes MAFIA and GPT [2]. From extensive parameter studies an optimized design has been derived [3] and construction of the gun and diagnostics have recently been completed. We report on the commissioning of the test stand and present first measurement results.

TEST STAND SETUP

DC Gun

The DC gun is a diode structure with a cathode electrode on -100 kV DC potential with respect to the grounded anode. The cathode electrode has at its center a 1.5 mm diameter insertion port for the FEA which has an active radius of 500 μm. The FEA has a gate layer which is connected to the pulser in the HV deck; the pulser can deliver 320 V (with respect to the FEA potential) pulses with 5 ns minimum pulse length. The gun geometry has been optimized for minimum emittance at its exit while keeping the accelerating gap large enough ($\approx$ 11 mm) to avoid peak electric field strength larger than 20 MV/m on the anode iris. The anode iris has a diameter of 1.5 mm which allows the beam to pass without particle loss. The modular design of the test stand gun allows simple exchange of the anode and cathode electrodes without disassembling or redesigning the entire test stand.

Solenoid Magnet

In order to focus the beam and to compensate space-charge blow-up an in-vacuum DC solenoid magnet has been designed and installed right behind the anode structure. The solenoid's 1000 copper windings are capable of delivering 200 mT of magnetic field strength on axis [4]. It is actively cooled by an in-vacuum water circuit dissipating roughly 50W of heat from within the iron yoke case. Through proper tuning of the solenoid current with the digital power supply beam foci can be produced at any location within the diagnostic module which is built around a 433 mm long drift section behind the solenoid magnet.

Diagnostic Module

The diagnostic module consists of a YAG screen, Faraday cup, slit and pinhole arrays, pepper pot, P43 phosphor screen, CCD cameras, and a set of motors capable of driving these devices into their proper positions. The diagnostic devices are controlled and their data acquisition read out through EPICS which is used as the test stand control system.

The 30 mm diameter YAG screen with CCD camera and zoom optics can be inserted into the beam from the side in order to visualizes the transverse beam distribution at the location of the slit and pinhole arrays. The coaxial Faraday cup can inserted right behind the solenoid magnet; it has a diameter of 20 mm and offers high bandwidth ($>$ 4 GHz). The charge and time structure of the bunches emitted from the FEA are read out with a 2 GHz, 20 GS/s digital oscilloscope.

From the top and side two mask holders can be inserted in the beam path. Each holder carries three masks: a single slit, an array of slits, and a pepper pot. The slit width is 20 μm, the pitch between slits is 170 μm; the pepper pot hole diameter is 50 μm, the distance pitch holes is 320 μm. The masks are laser eroded substrates of 100 μm tungsten. The position of the masks is measured by linear encoders with a resolution of 0.5 μm. In order to visualize the beamlets that pass the slit(s) or pinholes there is a phosphor screen inserted from the back and a CCD camera with variable zoom optics; the ultimate optical resolution of this system is $\approx$ 3 μm [5]. The phosphor screen is optimized for 100 keV electrons; its thickness is 6–8 μm, the granularity is roughly 3 μm and the substrate is aluminized.

The slit/pinhole arrays and pepper pot will allow two principal measurement modes: Without solenoid focussing the moveable pepper pot arrangement (300 mm travel) will allow imaging of diverging beamlets emerging from various longitudinal positions onto the phosphor screen at a fixed 300 mm distance. With proper solenoid focussing a beam focus can be placed at the location of the slits or pinhole arrays. In this regime the phosphor screen can be moved (300 mm travel) with respect to the slits or holes in order to ensure proper resolution of each beamlet on the screen. Both modes should deliver spacial and angular dimensions of the beam at the location of the slits or holes and allow a comparison of results.

FEA PERFORMANCE

The first FEA being used at the test stand is a Spindt-type gated array with molybdenum nano-tips from SRI International; the active area has a 1 mm diameter. The cathode surface is mounted on a TO-5 header containing electrical leads to the gate and tip layers. It has been observed that the FEAs are very sensitive to vacuum conditions and that HV breakdown normally leads to destruction of parts of the gate layer and tips resulting in a bridged and non-functional FEA. If one manages to step up the HV without experiencing breakdown (presently a maximum of 60 kV has been reached), FEA emission can be triggered by pulsing the gate layer with respect to the tips

Fig. 1 shows charge and peak current measured on the Faraday cup as a function of the applied gate voltage for a 100 ns gate pulse at 40 kV DC HV. The gate voltage was not increased beyond 200 V because strong fluctuations and bursts of the emitted current were observed at this level; such bursts normally precede a discharge from tips to gate which can trigger HV breakdown and ultimately destroy the FEA. At this gate voltage level a saturation of the emitted current (due to space-charge limitation of the cathode) can not be observed. The maximum peak currents obtained are well below the originally targeted 100 mA. Thus the repulsive space-charge forces within the bunch are dramatically reduced and the gun design becomes inherently over-focussing. In addition such a beam is emittance dominated rather than space charge dominated which does not allow proper investigation of emittance compensation.

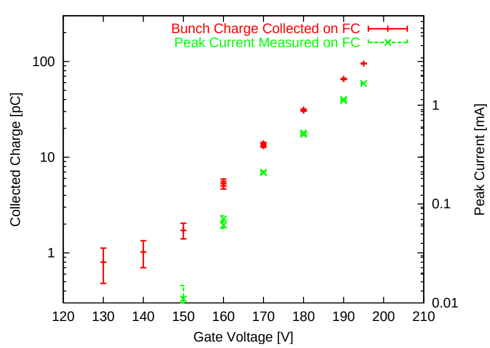

Figure 1: FEA calibration at 40kV DC HV with 100 ns pulses.

Transverse beam size measurements done with the phosphor screen and CCD camera show that the beam enters the solenoid immediately after reaching a 0.1 mm waist due to the electrostatic over-focussing. The solenoid is thus only capable of producing a beam waist within a few cm of its exit.

EMITTANCE MEASUREMENTS

Several methods are used at the test stand to measure the transverse bunch emittance. By measuring the beam size as a function of the solenoid current, the emittance and twiss parameters can be derived. If a single slit is inserted into the beam, the beam size at this location is known and the resulting beamlet size is measured downstream, the emittance can be deduced. If an array of parallel slits is hit by the beam, the emerging beamlets can be imaged downstream which renders the emittance and phase space distribution. Finally, if instead of a slit array a pinhole array is used the measurement can be done for both transverse planes in a single shot.

Solenoid Scan

The solenoid scan is similar to the quadrupole scan technique, but makes use of the focussing properties of a solenoid magnet instead of a quadrupole. Since the test stand beam is rotationally symmetric, the solenoid can be treated as a purely focussing element in both planes with a focussing strength given by $k = (B/(2p/e))^2$ where B is the mean longitudinal magnetic field $B = (\int B\,ds)/l_{\mathrm{eff}}$ generated by the solenoid. It can be shown that in thin lens approximation $\sigma^2_{x,y}$ downstream of the solenoid is a parabolic function in k. From a quadratic fit the emittance and twiss parameters at the solenoid location can be derived. Furthermore, error propagation can be calculated analytically delivering an exact error contribution in the final emittance result.

An example for a solenoid scan emittance measurement is given in Fig. 2. The beam is imaged on the phosphor screen 137 mm downstream of the solenoid and the horizontal beam size σ_x is measured as a function of the solenoid current. The emittance and twiss parameters are calculated from the fit parameters of the parabola. The measurement was repeated for several different bunch charges; the results are shown in Fig. 3.

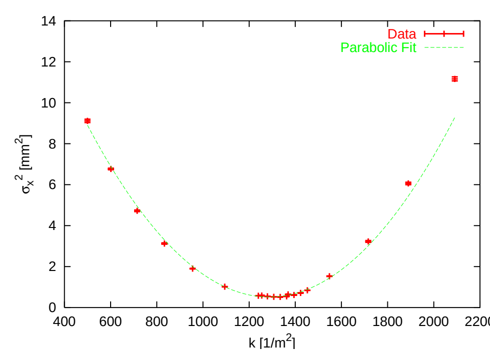

Figure 2: Solenoid scan data taken at 40 kV DC HV, with 40 pC bunch charge. The beam size measurement was done by averaging over ten shots in order to enhance the SNR. The results are $\varepsilon_n = (5.883 \pm 0.237) \cdot 10^{-7}$ m rad, $\beta = (0.233 \pm 0.016)$ m, $\alpha = (-5.783 \pm 0.364)$.

Slit and Pinhole Measurements

Due to the presently weak bunch current several phosphor images have to be averaged in order to get a decent

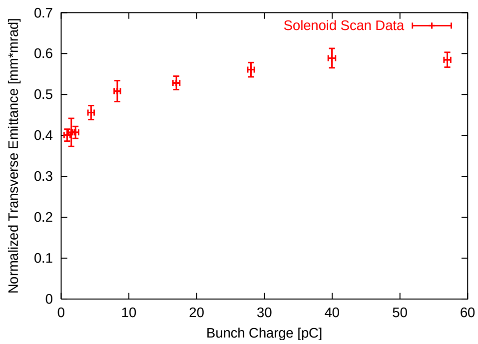

Figure 3: Emittance as a function of bunch charge. The emittance was measured with a solenoid scan at 40 kV DC HV, with 100 ns bunches and by averaging over ten shots in order to enhance the SNR.

SNR. Otherwise, slit and pinhole array measurements can deliver single shot emittance measurement and phase space reconstruction whereas the solenoid scan requires several shots to measure emittance and twiss parameters.

At the location of the single slit, the YAG screen monitor is used to measure the transverse beam size; the size of the downstream image of the emerging beamlet can be used to calculate the emittance according to $\varepsilon_x = \sqrt{\langle x^2\rangle \cdot \langle x\prime^2\rangle}$ where $\langle x^2\rangle$ is the RMS beam size measured at the position of the slit and $\langle x\prime^2\rangle$ is the uncorrelated divergence spread derived from the beamlet image size σ_x with $\langle x\prime^2\rangle = \sigma_x^2/L^2$ where it is assumed that the beamlet image is much larger than the slit width. For a bunch charge of 40 pC and a solenoid setting of B_z = 47.3 mT the RMS beam size at the location of the slit is (0.725 $\pm$ 0.073) mm. The measured beamlet RMS width on the screen is (0.138 $\pm$ 0.008) mm. The distance from slit to screen is 39 mm. This results in an emittance of ε_x = (2.54 $\pm$ 0.29)$\cdot 10^{-6}$ m rad. The slit measurement results are consistently higher than the solenoid scan and pinhole results which is presently under investigation.

For slit and pinhole arrays the measurement is similar, but beam size at the location of the array is not required. A very lucid illustration of how emittance, twiss parameters and phase space density are calculated from the images of the emerging beamlets is given in [6]. The (uncentered) divergence centroid and divergence spread for slit position i is given by $\overline{x}_i\prime = \langle x_i - \overline{x}_i\rangle/L$ and $\sigma_i\prime = \sqrt{\langle(x_i - \overline{x}_i)^2\rangle/L^2 - (\overline{x}_i\prime)^2}$.

Due to the large divergence of the low-current beam emitted by the present FEA, the slit array beamlet images overlap. The pitch between the slits would have to be increased in order to properly resolve the large divergence. The pinhole arrays have a larger pitch and can be used for fairly defocussed beams where the beamlet overlap is reduced. On the other hand, the large beam size leads to a reduced SNR. The resulting emittance is very sensitive on high background levels and overlapping hole images. A pinhole array image is shown in Fig. 4.

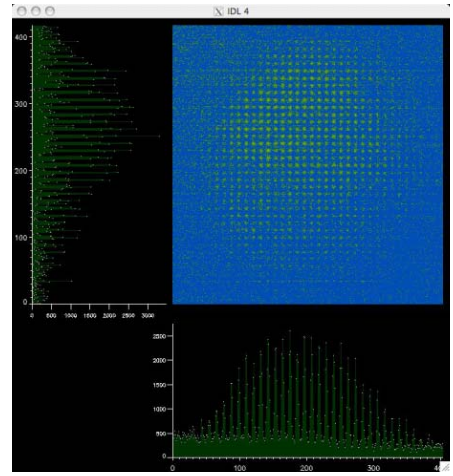

Figure 4: Pinhole array measurement for a bunch charge of 56 pC and a solenoid setting of B_z = 25.7 mT. In order to increase the SNR the image integrates over 25 shots. The distance from slit to screen is 39 mm. This results in emittances of ε_x = (1.47 $\pm$ 0.29) $\cdot 10^{-6}$ m rad and ε_y = (2.14 $\pm$ 0.43) $\cdot 10^{-6}$ m rad.

OUTLOOK

The test stand diagnostics deliver a full transverse phase space characterization of the FEA-based beam. In the scope of the LEG project, improved FEAs are required. Inhouse fabrication of FEAs optimized for use as electron sources has started: Higher bunch charges will improve the SNR allowing single shot measurements. By introducing a focussing layer in addition to the gate layer, the initial divergence spread will be reduced. Together with the increased beam size at solenoid entry (due to the increased bunch charge), the solenoid should be able to properly focus the beam at the location of the diagnostic equipment as originally intended.

REFERENCES

[1] The Low Emittance Gun Project at PSI, http://leg.web.psi.ch.

[2] A. E. Candel, M. M. Dehler, S. C. Leemann, ”Electron Beam Dynamics Simulations for the Low Emittance Gun”, EPAC’04, July 2004, Lucerne, p. 2505.

[3] S. C. Leemann, ”100 keV Gun Test Stand: Design and Parameter Study”, PSI/SLS Internal Report, May 2004, http://slsbd.psi.ch/pub/slsnotes/tmeta040244.pdf.

[4] S. C. Leemann, Å. Andersson, ”Gun Test Stand Solenoid Measurements”, PSI/SLS Internal Report, April 2005, http://slsbd.psi.ch/pub/slsnotes/tmeta050264.pdf.

[5] Å. Andersson, S. C. Leemann, ”Experimental Determination of the Point-Spread Function for the Optical Diagnostics Setup at the 100 keV Gun Test Stand”, PSI/SLS Internal Report, September 2005, http://slsbd.psi.ch/pub/slsnotes/tmeta050278.pdf.

[6] S. G. Anderson et al., ”Space-charge effects in high brightness electron beam emittance measurements”, Phys. Rev. ST Accel. Beams, Vol. 5 (2002) 014201.